Precision Neutron Interferometric Measurement of the *nd* Coherent Neutron Scattering Length and Consequences for Models of Three-Nucleon Forces

T. C. Black,[1] P. R. Huffman,[2] D. L. Jacobson,[2] W. M. Snow,[3] K. Schoen,[4] M. Arif,[2] H. Kaiser,[4]
S. K. Lamoreaux,[5] and S. A. Werner[4,2]

[1]*University of North Carolina at Wilmington, Wilmington, North Carolina 28403-3297*
[2]*National Institute of Standards and Technology, Gaithersburg, Maryland 20899-8461*
[3]*Indiana University/IUCF, Bloomington, Indiana 47408*
[4]*University of Missouri–Columbia, Columbia, Missouri 65211*
[5]*Los Alamos National Laboratory, Los Alamos, New Mexico 87545*
(Received 19 November 2002; published 16 May 2003)

We have performed the first high precision measurement of the coherent neutron scattering length of deuterium in a pure sample using neutron interferometry. We find $b_{nd} = (6.665 \pm 0.004)$ fm in agreement with the world average of previous measurements using different techniques, $b_{nd} = (6.6730 \pm 0.0045)$ fm. We compare the new world average for the *nd* coherent scattering length $b_{nd} = (6.669 \pm 0.003)$ fm to calculations of the doublet and quartet scattering lengths from several modern nucleon-nucleon potential models with three-nucleon force (3NF) additions and show that almost all theories are in serious disagreement with experiment. This comparison is a more stringent test of the models than past comparisons with the less precisely determined doublet scattering length of $^{2}a_{nd} = (0.65 \pm 0.04)$ fm.

PACS numbers: 21.30.–x, 03.75.Dg, 21.45.+v, 25.40.Dn

The nature of three-nucleon forces (3NF) has been an especially active area of study in nuclear physics over the last decade and a half [1]. Nonetheless, the current models are incomplete and have a tendency to resolve discrepancies in some observables at the expense of exacerbating discrepancies in others [2,3]. In this Letter, we present a new measurement of the coherent *nd* scattering length, b_{nd}, which can be used as part of a stringent program of tests of nucleon-nucleon (NN) and 3NF models. We show that almost all modern NN potentials, including those with parametric 3NF adjusted to replicate the triton binding energy, disagree with the new world average value of b_{nd}.

The present family of modern NN potentials—AV18 [4], CD-Bonn [5], and the various Nijmegen potentials [6]—fit the extensive database of NN bound state properties and scattering observables to within the precision of the data. More recent potential models based on chiral perturbation theory predict NN properties and observables with comparable accuracy [7,8]. There is growing confidence that the NN interaction is understood well enough that deviations from NN force model predictions in 3N observables for which relativistic corrections are negligible can confidently be interpreted as 3NF effects.

The simplest systems that exhibit 3NF effects are the bound states of ^{3}H and ^{3}He and the scattering states of *nd* and *pd*. Since ^{3}H and *nd* are free from long-range electromagnetic interactions that complicate both theory and experiment, they are the systems of choice for precision tests at low energy. The computational tools presently available to analyze these systems are believed to be excellent.

The 3N interactions employed in realistic calculations have evolved to reconcile a growing number of discrepancies between theoretical and experimental observables [9]; the nucleon binding energies, the nucleon-deuteron (Nd) doublet scattering lengths, the Nd vector analyzing power A_y at low energies [10], and Nd spin observables above the deuteron breakup threshold [11]. Although the trinucleon binding energy and the Nd doublet scattering lengths a_{Nd} have been observed to be computationally correlated, as shown in the well-known Phillips lines, they are not equivalent. The doublet scattering length has special importance for effective field theory calculations of 3N observables. A momentum cutoff parameter required in the renormalized theory can be adjusted to match the experimental value of $^{2}a_{Nd}$ [12], which then forms the fundamental expansion parameter for the system in this channel [13].

The *nd* bound state coherent scattering length b is the forward scattering amplitude due to the strong interaction from an unpolarized ensemble in the limit of zero neutron energy. It is simply related to the free nuclear doublet and quartet scattering lengths $^{2S+1}a_{nd}$ [14]

$$b_{nd} = \left(\frac{m_n + m_d}{m_d}\right)\left[(\tfrac{1}{3})\,^{2}a_{nd} + (\tfrac{2}{3})\,^{4}a_{nd}\right], \qquad (1)$$

where m_n and m_d are the neutron and deuteron masses.

Using the Neutron Interferometer and Optics Facility (NIOF) at NIST [15], we have measured b_{nd} using a pure D$_2$ gas sample. Since the quartet scattering length can be accurately calculated from NN potentials and is largely determined by deuteron properties and therefore insensitive to 3NF effects, we believe that comparison to the

coherent nd scattering length is a more stringent test of NN + 3NF models than comparison to the doublet scattering length. Moreover, since the effective range function in the quartet spin channel is a smooth function of energy, the quartet scattering length can be accurately extracted from an energy dependent phase shift analysis [16], so that both theoretically and experimentally, knowledge of the bound coherent scattering length is equivalent to knowledge of the doublet scattering length.

In neutron interferometry [14], the phase shift of the neutron beam due to the optical potential of a material is measured. To high accuracy, the phase shift due to the sample is

$$\Delta \phi = (n_r - 1)kD_{\text{eff}} = -\sum_l \lambda N_l b_l D_{\text{eff}}, \qquad (2)$$

where n_r is the real part of the index of refraction, $(n_r - 1) \approx 10^{-5}$, k is the wave vector, and the sum is taken over the elemental species. To measure the bound coherent scattering length b to 0.05% absolute accuracy, measurements of the neutron optical phase shift $\Delta\phi$, the atom density N_l, the sample thickness D_{eff}, the neutron wavelength λ, and the gas purity, at the 0.02% level are required.

Measurements were performed using a perfect crystal silicon neutron interferometer with high phase contrast (80%) and long-term phase stability ($\approx 5°$ per day) [15]. The single crystal interferometer is schematically illustrated in Fig. 1. A monochromatic cold neutron beam ($E = 11.1$ meV, $\lambda = 0.271$ nm, $\Delta\lambda/\lambda \leq 0.5\%$) is coherently divided near point A by Bragg diffraction into two beams that travel along paths I and II. These beams are again split near points B and C and are coherently recombined to interfere near point D.

The phase shift, $\Delta\phi$, is measured by a secondary sampling method in which a phase shifter is positioned across both beams. The intensities of the O and H beams
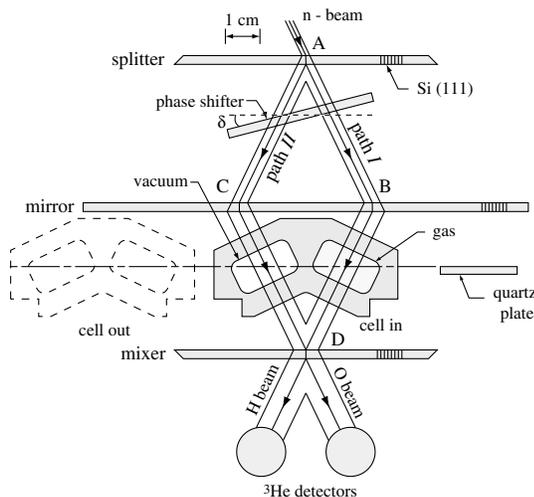

FIG. 1.   A schematic view of the Si perfect crystal neutron interferometer with gas cell and quartz alignment flag. Individual components are discussed in the text.

as a function of the phase flag angle, δ, can be described by the following relations:

$$\begin{aligned} I_O(\delta) &= A_O + B\cos[C\xi(\delta) + \Delta\phi_0], \\ I_H(\delta) &= A_H + B\cos[C\xi(\delta) + \Delta\phi_0 + \pi]. \end{aligned} \qquad (3)$$

The function $\xi(\delta)$ is the path length difference of the two beams (I and II) traversing the phase flag. The parameters A_O, A_H, B, C, and $\Delta\phi_0$ are extracted from fits to the data. The value of $\Delta\phi_0$ and its corresponding uncertainty is used to determine the phase difference between the two interfering beams.

In order to minimize the effect of the phase shift due to the aluminum cell, the cell walls were designed to extend across both beam paths, producing compensating phase shifts. When the cell is perfectly aligned, the beams strike both cell compartments perpendicular to their surfaces, minimizing systematics. The resulting cell phase shift was 5 times smaller than the gas phase shift, reducing the relative contribution of the cell to the total phase shift uncertainty to 1.7×10^{-4}. Alignment of the cell was performed by a phase shift measurement using a quartz plate mounted on the kinematic mount of the cell, similar to the procedure used in Ref. [17].

Gas was then introduced into the chamber on path I, while the cell on path II was evacuated. Interferograms with the cell first in the beam and then translated out of the beam were collected to determine the phase shift due to the gas and to the small difference in aluminum thickness. This phase difference is combined with measurements of N, D_{eff}, λ, and the gas purity to extract b_{nd}.

The atom density N is determined using the ideal gas law with virial coefficient corrections up to the third pressure virial coefficient. For deuterium, the virial coefficients have been measured with sufficient accuracy to determine N with a relative uncertainty of 0.001% [18,19]. The absolute temperature was measured using two calibrated 100 Ω platinum thermometers which have an absolute accuracy of 0.023% at 300 K. The pressure was measured using a silicon pressure transducer capable of measuring the absolute pressure to better than 0.01%.

The gas cell was (1.0016 ± 0.0001) cm thick at an absolute temperature of (20.00 ± 0.05) °C. Dimensional changes in the cell due to the ≈ 12 bars pressure result in a change in thickness at the center of the cell of less than 1 μm, which amounts to a systematic effect on the thickness of less than 0.01%.

Both mass spectroscopy and Raman spectroscopy were employed to measure impurities in the D_2 gas sample, with the primary contaminants being HD and D_2O. The mole fractions of D, H, and O were measured to be $x_D = 0.998\,40 \pm 0.000\,17$, $x_H = 0.001\,500 \pm 0.000\,065$, and $x_O = 0.000\,050 \pm 0.000\,016$. The expression for b_{nd}, corrected for impurities, is $b_{nd} = [b_{\text{gas}} - b_H x_H - b_O x_O]/x_D$, where $b_H = (-3.746 \pm 0.0020)$ fm and $b_O = (5.805 \pm 0.004)$ fm [20]. Corrections due to the molecular
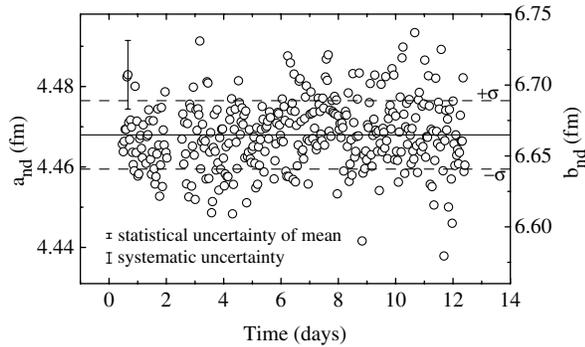
FIG. 2. Values for the coherent scattering length on a run-to-run basis.

state of the gas are not relevant within the reported accuracy of the measurement.

The neutron wavelength was measured using an analyzer crystal placed in the H-beam as described in Ref. [21]. Rotating this crystal through both the symmetric and antisymmetric Bragg reflections allows the absolute Bragg angle, θ_B, to be determined to high accuracy, yielding $\lambda = (0.271\,266 \pm 0.000\,012)$ nm. The stability of the wavelength over time was shown in a separate test to be better than 0.001%.

The value of b_{nd} was extracted for each 42 min data set on a run-by-run basis (Fig. 2). These values were then averaged to obtain the coherent neutron scattering length $b_{nd} = (6.665 \pm 0.004)$ fm. To compare this value with the previous world average value of b_{nd}, we consulted the existing compilations of previous measurements [20,22] and excluded all measurements which were not published in a refereed journal and all measurements which were later retracted. The remaining values were combined into an average with results weighted by the inverse square of their uncertainties in the usual manner [23]. The values are presented in Fig. 3. The result of this evaluation is $b_{nd} = (6.6730 \pm 0.0045)$ fm with a reduced $\chi^2 = 0.6$. Our value, $b_{nd} = (6.665 \pm 0.004)$ fm, is consistent with the previous world average and of comparable precision. The new world average value for the bound nuclear scattering length of deuterium is $b_{nd} = (6.669 \pm 0.003)$ fm.

For the forward scattering, which is the only component that contributes to the phase shift seen by the interferometer, the scattering amplitudes from both the Mott-Schwinger and neutron-electron interactions are zero [14]. The size of the scattering due to the electric polarizability of the neutron is less than $-0.000\,017$ fm [24]. This measurement is thus sensitive only to the same nuclear interactions that are calculated in theoretical models of 3N scattering.

To illustrate the impact of comparing theoretical calculations to the precision data on the coherent scattering length, a number of modern calculations of the nd scattering lengths are shown in Table I. The dependence of the theoretically calculated $^2S_{1/2}$ scattering length on the inclusion of a 3NF is clearly seen. We note that, as expected, none of the theories which do not incorporate a 3NF come close to matching the nd coherent scattering length. The MTI-III model, which gives fair agreement without a 3NF, nonetheless fails to reproduce the NN partial wave phase shifts. Of the potential models that include a 3NF, only the AV14 potential with the Brazil 3NF [27] and the AV14 potential with the TM 3NF [30] are in agreement with the data, as shown in Fig. 4. We stress that the precision with which the coherent nd scattering length is known can, in concert with the triton binding energy, set tight constraints on NN potential models as well as on 3BF models. None of the potential models listed in Table I, for example, include charge independence breaking (CIB) effects. The authors of a recent paper [31] estimate that CIB effects increase the nd
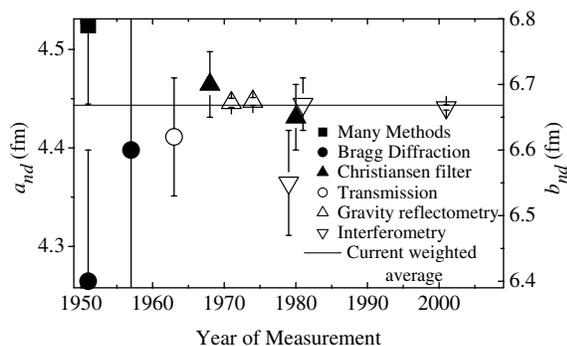

FIG. 3. Bound coherent neutron scattering length for nd along with reported uncertainties. Our result for D_2 value is consistent with the previous and the current world averages.

TABLE I. Theoretical calculations of the nd scattering lengths. The rightmost column is the coherent scattering length. The 3NF parameters in the boldfaced potential models have been adjusted to reproduce the triton binding energy.

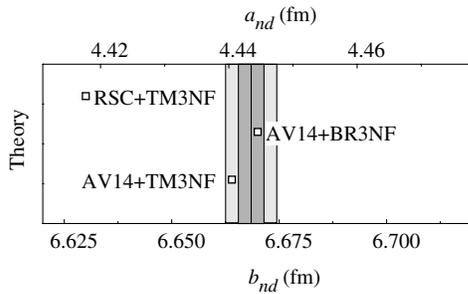| Ref.	Potential model	$^2a_{nd}$ (fm)	$^4a_{nd}$ (fm)	a_{nd} (fm)
[25]	MT I–III	0.70	6.44	4.52
[26]	AV14	1.35	6.38	4.70
	SSCC	1.32	6.41	4.71
[27]	RSC	1.52	6.302	4.71
	RSC + TM3NF	0.393	6.308	4.336
	AV14	1.200	6.372	4.648
	AV14 + BR3NF	0.001	6.378	4.252
	RSC + TM3NF	0.657	6.304	4.422
	AV14 + BR3NF	0.567	6.380	4.442
[28]	MT I–III	0.71	6.43	4.52
[29]	MT I–III	0.702	6.442	4.529
	AV14	1.196	6.380	4.652
[30]	AV14	1.189	6.379	4.649
	AV14 + TM3NF	0.5857	6.371	4.443

FIG. 4. Theoretical calculations of the coherent scattering length compared with the new world average. The central dark band is the 1σ confidence band, and the lighter band is the 2σ confidence band.

doublet scattering length by 0.19 fm. Arriving at a simultaneously correct NN and 3N potential model requires sufficient precision in all relevant fundamental low-energy parameters, especially the triton binding energy and the coherent nd scattering length.

We observe that none of the theories, with the exception of the AV14 potential with a 3N force, are in agreement with the precisely known world average coherent nd scattering length of $a_{nd} = (4.443 \pm 0.002)$ fm. The precision of the measurement of this critical parameter is now such that we can distinguish between different theoretical combinations of NN and 3NF models, even when the 3N forces have been adjusted to replicate the triton binding energies. Relativistic corrections to the triton binding energy, which were shown by the authors of [32] to weaken the binding by 0.29–0.43 MeV, further reduce the correlation between b_{nd} and the triton binding energy, and provide another justification for using this pair of parameters to perform rigorous tests of NN and 3NF models. Clearly the theoretical community now has an incentive to systematically investigate nuclear force models for these parameters with comparable accuracy, especially since the precision of interferometric measurements of neutron-nucleus scattering can be extended by at least an order of magnitude.

[1] L. Canton and W. Schadow, Phys. Rev. C **62**, 044005 (2000).
[2] J. Kuroś-Żołnierczuk, H. Witała, J. Golak, H. Kamada, A. Nogga, R. Skibiński, and W. Glöckle, Phys. Rev. C **66**, 024003 (2002).
[3] W. Glöckle, H. Witała, D. Hüber, H. Kamada, and J. Golak, Phys. Rep. **274**, 107 (1996).
[4] R. B. Wiringa, V. G. J. Stoks, and R. Schiavilla, Phys. Rev. C **51**, 38 (1995).
[5] R. Machleidt, Phys. Rev. C **63**, 024001 (2001).
[6] V. G. J. Stoks, R. A. M. Klomp, C. P. F. Terheggen, and J. J. deSwart, Phys. Rev. C **49**, 2950 (1994).
[7] D. R. Entem and R. Machleidt, Phys. Lett. B **524**, 93 (2002).
[8] E. Epelbaum, H. Kamada, A. Nogga, H. Witała, W. Glöckle, and Ulf-G. Meißner, Phys. Rev. Lett. **86**, 4787 (2001).
[9] S. C. Pieper, V. R. Pandharipande, R. B. Wiringa, and J. Carlson, Phys. Rev. C **64**, 014001 (2001).
[10] W. Tornow and H. Witała, Nucl. Phys. **A637**, 280 (1998).
[11] E. J. Stephenson, H. Witała, W. Glöckle, H. Kamada, and A. Nogga, Phys. Rev. C **60**, 061001 (1999).
[12] W. Dilg, L. Koester, and W. Nistler, Phys. Lett. **36B**, 208 (1971).
[13] P. F. Bedaque, H. W. Hammer, and U. van Kolck, Phys. Rev. Lett. **82**, 463 (1999).
[14] H. Rauch and S. Werner, *Neutron Interferometry: Lessons in Experimental Quantum Mechanics* (Oxford University Press, New York, 2000).
[15] M. Arif, D. E. Brown, G. L. Greene, R. Clothier, and K. Littrell, Proc. SPIE Int. Soc. Opt. Eng. **2264**, 21–26 (1994).
[16] T. C. Black, H. J. Karwowski, E. J. Ludwig, A. Kievsky, M. Viviani, and S. Rosati, Phys. Lett. B **471**, 103 (1999).
[17] A. Ioffe, D. L. Jacobson, M. Arif, M. Vrana, S. A. Werner, P. Fischer, G. L. Greene, and F. Mezei, Phys. Rev. A **58**, 1475 (1998).
[18] A. Michels, W. de Graaff, T. Wassenaar, J. M. H. Levelt, and P. Louwerse, Physica Grav. **25**, 25 (1959).
[19] J. H. Dymond, *The Virial Coefficients of Pure Gases and Mixtures: A Critical Compilation* (Oxford University Press, New York, 1980).
[20] L. Koester, H. Rauch, and E. Seymann, At. Data Nucl. Data Tables **49**, 65 (1991).
[21] K. C. Littrell, Ph.D. thesis, University of Missouri, 1997.
[22] H. Rauch and W. Waschkowski, in *Elementary Particles, Nuclei, and Atoms*, edited by H. Schopper, Landolt-Bornstein, New Series, Group I, Vol. 16, Pt. A (Springer, Berlin, 2000), Chap. 6.
[23] K. Hagiwara *et al.*, Phys. Rev. D **66**, 010001 (2002).
[24] J. Schmiedmayer, P. Riehs, J. A. Harvey, and N. W. Hill, Phys. Rev. Lett. **66**, 1015 (1991).
[25] J. L. Friar, B. F. Gibson, and G. L. Payne, Phys. Rev. C **28**, 983 (1983).
[26] J. L. Friar, B. F. Gibson, G. L. Payne, and C. R. Chen, Phys. Rev. C **30**, 1121 (1984).
[27] C. R. Chen, G. L. Payne, J. L. Friar, and B. F. Gibson, Phys. Rev. C **44**, 50 (1991).
[28] C. R. Chen, G. L. Payne, J. L. Friar, and B. F. Gibson, Phys. Rev. C **39**, 1261 (1989).
[29] A. Kievsky, M. Viviani, and S. Rosati, Nucl. Phys. **A577**, 511 (1994).
[30] A. Kievsky, Nucl. Phys. **A624**, 125 (1997).
[31] E. Epelbaum, A. Nogga, W. Glöckle, H. Kamada, Ulf-G. Meißner, and H. Witała, Phys. Rev. C **66**, 064001 (2002).
[32] H. Kamada, W. Glöckle, J. Golak, and Ch. Elster, Phys. Rev. C **66**, 044010 (2002).